

Study of Heat Pipe Performance with Water/ Water-Based Nanofluid

دراسة الأداء لأنبوب حراري باستخدام الماء/ الماء و به جزيئات فائقة الدقة

M. G. Mousa, E. A.M. Elshafei and Osama M. Hamed

Mechanical Power Eng. Dept., Faculty of Engineering, Mansoura Univ., Mansoura, Egypt.

Email: Mgmousa@mans.edu.eg and eelshafei@mans.edu.eg

المخلص العربي

في هذا البحث تمت دراسة الأداء الحراري لأنبوب حراري أفقي باستخدام مائعي تبريد مختلفين (ماء و ماء +جزيئات فائقة الدقة من أكسيد ألومونيوم بتركيزات مختلفة). وتمت الدراسة تحت ظروف تشغيل مختلفة من حيث نسبة الامتلاء للمائع داخل المبخر ومعدل التسخين الحراري لبيان تأثير تلك الظروف على كل من معامل انتقال الحرارة الكلي التوسط وكذلك المقاومة الحرارية الكلية للأنبوب الحراري وأظهرت الدراسة أن التحسين في معامل انتقال الحرارة الكلي في حالة استخدام مائع ذو جزيئات فائقة الدقة بالنسبة إلى قيمته باستخدام الماء كوسيط تبريد في حدود 10.5% إلى 37% . وتم إيجاد علاقة مصطلحية للربط بين المتغيرات المؤثرة في أداء الأنبوب الحراري. وتم كذلك مقارنة النتائج بنظيرتها من الأبحاث السابقة ووجد توافق إلى حد ما مع مناقشة أسباب الحيدود بينهما.

Abstract

Thermal performance of a flat heat pipe cooling system is experimentally investigated. Pure water and Al₂O₃-water based nanofluid are used as working fluids. An experimental setup is designed and constructed to study its performance under different operating conditions. The effect of working fluid, filling ratio, volume fraction of nano-particle in the base fluid, and heat input rate on the average heat transfer coefficient and in turn the average Nusselt number are investigated. Total thermal resistance of the heat pipe for pure water and Al₂O₃-water based nanofluid are also predicted. Correlation is obtained to predict the influence of Prandtl number, filling ratio and dimensionless heat coefficient, K_q for Nusselt number. Results showed that the average heat transfer coefficient, using Al₂O₃-water based nanofluid enhanced by 10.5% up to 37% compared to that of pure water, depending on filling ratio and volume fraction of nano-particles in the base fluid. The experimental data are compared with the available literature and discrepancies between results are discussed.

Keyword: Flat Heat Pipe, Thermal Performance, Nanofluids, Cooling of Electronic Devices

Nomenclature

A	Surface area, m ²
FR	Filling ratio
H _e	Evaporator height, m
I	Electric current, Amp
k	thermal conductivity, W/m.K
L ₁	Characteristic length, m
N	Number of thermocouples
Q	Input heat rate, W
q	Heat flux, W/m ²
R	Total thermal resistance of heat pipe, K/W
T	Temperature, K
U	Overall heat transfer coefficient, W/m ² .K
V	Applied voltage, Volt
X	Horizontal coordinate parallel to the test section

Greek Symbols

φ	Volume fraction of nano-particles, %
ρ	Density, kg/m ³
μ	Dynamic viscosity, N.s/m ²

Subscript

a	Adiabatic
c	Characteristic
e	Evaporator
ef	Effective
l	Liquid
m	Base fluid
v	Vapor
W	Wall

Dimensionless Numbers

Nu	Nusselt number, $\frac{U \times L_1}{K_{ef}}$
RR	Reduction factor in thermal resistance, --
k_q	Dimensionless heat transfer, $\frac{Q}{K_{ef} \times L_1 \times \Delta T}$
Pr	Prandtl number, $\frac{\mu \times C_p}{K_{ef}}$

1. Introduction

Thermal density of electronic parts and systems has been increased continuously since high speed and high density are required for them. To solve this growing of heat generation by such electronic equipment, two-phase change devices such as heat pipe and thermosyphon cooling systems are now used in electronic industry and attracted the attention of several researchers [1].

Heat pipes are passive devices that transport heat from a heat source to a heat sink over relatively long distances via the latent heat of vaporization of a working fluid. The heat pipe generally consists of three sections; evaporator, the adiabatic section and the condenser. In the evaporator, the working fluid is evaporated as it absorbs an amount of heat equivalent to the latent heat of vaporization, while in the condenser section; the working fluid vapor is condensed and returns back to the evaporator. Nanofluids which are produced by suspending nano-particles with average sizes below 100 nm in traditional heat transfer fluids such as water and ethylene glycol are new working fluids that can be used in heat pipes. A very small amount of guest nano-particles, when dispersed uniformly and suspended stably in host fluids, can provide dramatic improvements in their thermal properties. The goal of using nanofluids is to achieve the highest possible thermal properties at the smallest possible volume fraction of the nano-particles (preferably < 1% and of particle size < 50 nm) in the host fluid.

Babin et al. [2], investigated analytically and experimentally the performance limitation and operating characteristics of micro heat pipe. A mathematical model described the distribution of the liquid in a micro heat pipe and its thermal characteristics was developed by Khrustalev and Faghri [3]. Longtin et al. [4], studied analytically one dimensional model of micro heat pipe to yield pressure, velocity and film thickness information along the length of the pipe. Results showed that, the maximum heat transfer capability of micro heat pipe varied with the inverse of its length and the cube of its hydraulic diameter. Hopkins et al.

[5], investigated analytically and experimentally heat transfer capabilities of two copper-water flat miniature heat pipes with diagonal trapezoidal micro capillary grooves and one copper-water flat miniature heat pipes with axial rectangular micro capillary grooves. Kim et al. [6], investigated experimentally and analytically a model for heat and mass transfer in a miniature heat pipe with a grooved wick structure. It was reported that the maximum heat transfer rate of 3 and 4 mm outer diameters heat pipe can be enhanced up to 48% and 73%, and the thermal resistance reduced by 7% and 11%, respectively. Lefevre and Lallemand [7], solved analytically both the liquid and vapor flows governing equations inside a flat micro heat pipe coupled with analytical solution for the temperature inside the micro heat pipe wall. Revellin et al. [8], investigated analytically a 2-D hydrodynamic model for both the liquid and the vapor phases and a 3-D thermal model of heat conduction inside a flat micro heat pipe wall. Joung et al. [9], investigated experimentally the performance of loop heat pipes with cylindrical and flat evaporators for diverse applications. Kaya et al. [10] developed a numerical model to simulate the transient performance characteristics of a loop heat pipe. Kang et al. [11], investigated experimentally the performance of a conventional circular heat pipe provided with deep grooves using nanofluid. The nanofluid used in their study was aqueous solution of 35 nm diameter silver nano-particles. It is reported that, the thermal resistance decreased by 10-80% compared to that of pure water.

Pastukhov et al. [12], experimentally investigated the performance of a loop heat pipe in which the heat sink was an external radiator cooled by air. It is reported that the use of additional means of active cooling in combination with loop heat pipe allows to increase the value of dissipated heat up to 180 W and to decrease the system thermal resistance down to 0.29 K/W. Chang et al. [13], investigated experimentally the thermal performance of a heat pipe cooling system with the thermal resistance model. An experimental investigation of thermosyphon thermal performance has been carried out using water

and dielectric heat transfer liquids as the working fluids was performed by Jouhara et al. [14]. The copper thermosyphon was 200 mm long with an inner diameter of 6 mm. Each thermosyphon was charged with 1.8 ml of working fluid and tested with an evaporator length of 40 mm and a condenser length of 60 mm. The thermal performance of the water charged thermosyphon outperformed the other three working fluids (FC-84, FC-77 and FC-3283) in both the effective thermal resistance as well as the maximum heat transport. However, these fluids, offered the advantage of being dielectric which may be better suited for sensitive electronics cooling applications. Furthermore, it provided adequate thermal performance up to approximately 50 W, after which liquid entrainment compromised the thermosyphon performance.

Lips et al. [15], studied experimentally the performance of flat plate heat pipe (FPHP). Temperature fields in the heat pipe were measured for different filling ratios, heat fluxes and vapor space thicknesses. Experimental results showed that the liquid distribution in the FPHP and thus its thermal performance depends strongly on both the filling ratio and the vapor space thickness. A small vapor space thickness induces liquid retention and thus reduces the thermal resistance of the system. Nevertheless, the vapor space thickness influences the level of the meniscus curvature radii in the grooves and hence reduces the maximum capillary pressure. As a result, it has to be carefully optimized to improve the performance of the FPHP. In all the cases, the optimum filling ratio was in the range of one to two times the total volume of the grooves. A theoretical approach, in non-working conditions, has been developed to model the distribution of the liquid inside the FPHP as a function of the filling ratio and the vapor space thickness.

Nanofluids are thought to be the next-generation heat transfer fluids due to their enhanced heat transfer performance compared to that when using traditional fluids. It offer stability compared to those of micro- or mill-sized particles and have a higher conductivity

than the host fluids themselves. These fluids are proposed for various uses in important applications, such as medical, electronics, coolant of automobiles, and HVAC [16]. Nanofluids with metallic and oxide nanoparticles have been investigated by several workers (Choi [17], Das et al. [18-19], and Lee et al. [20]), who found great enhancement of thermal conductivity (5-60%) over the volume fraction range of 0.1-5%. You et al. [21] found that nanofluids exhibited three-fold increase in critical heat flux of that for the base fluid. This parameter plays an important role in heat transfer where boiling is involved. All these features indicate the potential of nanofluids in applications involving heat removal. Issues concerning stability of nanofluids, have to be addressed before they can be put in use. Ironically, nanofluids of oxide particles are more stable but less effective in enhancing thermal conductivity in comparison with nanofluids of metal particles.

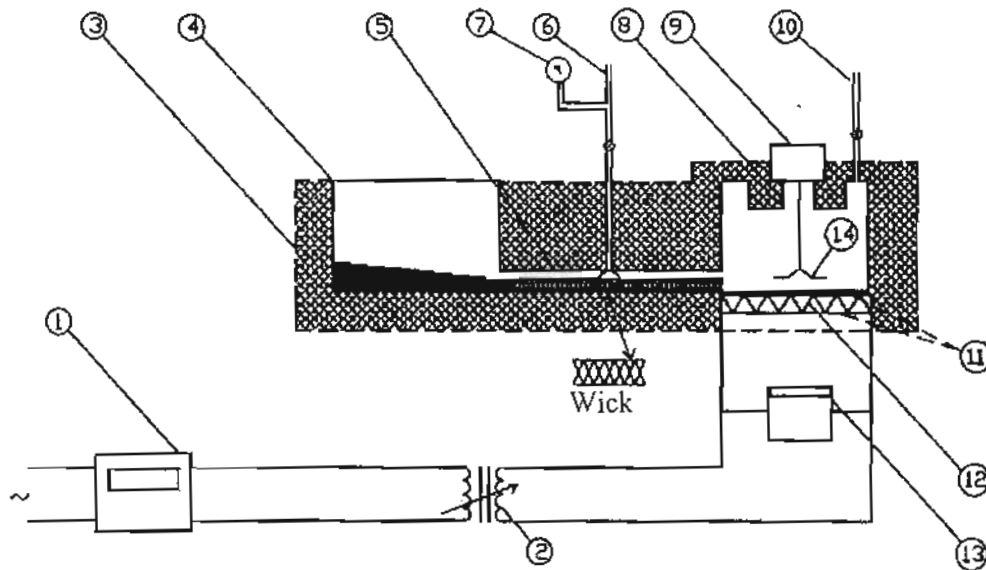
This article experimentally investigates the thermal performance of a flat heat pipe cooling system for electronic equipment. It aims to investigate the effect of different operating conditions on the thermal performance of the constructed heat pipe. These conditions involves the type of working fluid (pure water and Al_2O_3 -water based nanofluid); filling ratio of the working fluid; volume fraction of nano-particles in the base fluid, and heat input rate. Empirical correlation for its thermal performance taking into account the various operating parameters is also presented.

2. Experimental Setup and Procedure

This research adopts pure water and Al_2O_3 -water based nanofluid as working fluids. The nano-particles are of 40 nm in size. The test nanofluid is obtained by dispersing the nano-particles in pure water. A schematic layout of the experimental test rig is shown in Fig.1. The working fluid is charged through the charging line (6). In the heat pipe, the heat is generated by using an electric heater (12). The vapor generated in the evaporator (8) of $85 \times 50 \times 40$ mm, is moved towards the condenser (4) of $100 \times 50 \times 40$ mm via an insulated flat tube

(5). The condensate is allowed to return back to evaporator by capillary action "wick structure" through the flat tube. The surfaces of the evaporator, adiabatic section, and condenser sides are covered with 25 mm thickness of glass wool insulation (3). An electric motor (9) driving a paddle is used for circulating the nanofluid inside the evaporator to assure proper dispersion of nano-particles in their base fluid and to prevent its settling in the bottom of the evaporator during the experiments. 17 calibrated cooper-constantan thermocouples (T-type) are glued on the heat pipe surface and distributed along its length to measure the local temperature (see Fig.2). These thermocouples and that for measuring the ambient temperature

were connected to a digital temperature recorder via a multi-point switch. The non condensable gases are evacuated by a vacuum pump. The flat heat pipe is heated during vacuum pumping at 0.01 bar via the vacuum line (10). The power supplied to the electric heater (12) is measured by a multimeter (13). The input voltage was adjusted, using a variac autotransformer (2). The voltage drops across the heater were varied from 5 to 25 Volts. The A.C. voltage stabilizer (1) was used to ensure that there is no voltage fluctuation during the experiments. The pressure inside the evaporator was measured by a pressure gage with a resolution of 0.01 bar.



1. Stabilizer	2. Autotransformer	3. Insulation	4. Condenser	5. Adiabatic Section
6. Charge line	7. Pressure gage	8. Evaporator	9. Motor	10. Vacuum line
11. Mica sheet	12. Electric heater	13. Multi-meter	14. Paddle wheel	

Figure 1 Schematic layout of the test rig

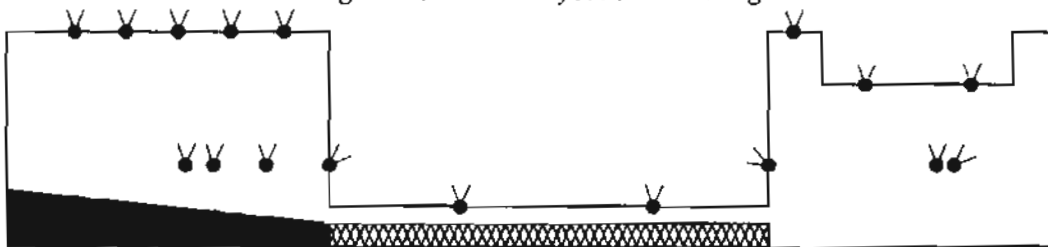


Figure 2 Thermocouples distribution along the heat pipe sections

In the experimental work, the effects of the type of working fluid, filling ratio, volume fraction of nano-particles in the base fluid, and heat input rate on the thermal performance of the flat heat pipe relying on natural convection are investigated. The experimental runs were executed according to the following steps:

1. The flat heat pipe is evacuated and charged with a certain amount of working fluid
2. The supplied electrical power is adjusted manually at the desired rate through the autotransformer.
3. As it was noted, the steady state condition was achieved after 1.0 hr running time, following the necessary adjustments for the input heat rate. Thereafter, the readings of thermocouples, voltage and internal pressure were recorded as follows:

Firstly, the readings of thermocouples, used for measuring the temperatures of the flat heat pipe surface and that for measuring the ambient temperature are recorded by changing the selector switch dial to meet all thermocouples one after another. Secondly, the voltages of the heater are measured to determine the value of applied heat flux. Finally, the pressure inside the evaporator is recorded

4. At the end of each run, power was changed to another value, and then from step 3 are repeated.
5. The flat heat pipe is then charged with another adjusted amount of working fluid (filling ratio, FR, follows as: 0.2, 0.4, 0.45, 0.50, 0.55, 0.60, 0.65, 0.70, 0.80 and 1.0, respectively). Then steps from 1 to 4 are repeated.
6. Considering Al_2O_3 -water based nanofluid as the working fluid, the volume fraction of nano-particles was changed as: 0.25%, 0.4%, 0.5%, 0.6%, 0.75%, 1.0% and 1.5% by volume, respectively. Then steps from 1 to 5 are repeated.

The 17 thermocouples (with the uncertainty lower than $0.20\text{ }^\circ\text{C}$) were distributed along the surfaces of the heat pipe sections as follows: Six thermocouples are attached to the evaporator; two thermocouples are attached to the adiabatic section and the rest of thermocouples (nine) are attached to the condenser section. The obtained data for temperatures and input heat rate were used to calculate the overall heat transfer coefficient and Nusselt number.

3. Data Reduction

Accurately characterizing the thermal power transfer, Q is a somewhat more complicated task because it is difficult to accurately quantify the energy loss to the ambient surroundings. The whole surface of the heat pipe was good insulated so that the rate of heat loss can be ignored. The heat input rate can be calculated using the supplied voltage and known current measurements of the multi-meter such that,

$$Q = I \times V \quad (1)$$

and the heat flux, q as;

$$q = \frac{Q}{A_e} \quad (2)$$

The experimental determination of the thermal performance of the heat pipe requires accurate measurements of evaporator and condenser temperatures as well as the power transferred along each. Characterizing the evaporator and condenser temperature is a relatively straightforward task and is obtained by simply averaging the temperature measurements along the evaporator and condenser surfaces which can be expressed as:

$$\bar{T}_e = \frac{\sum_{i=1}^{N_{te}} T_{ei}}{N_{te}}, \quad \bar{T}_c = \frac{\sum_{i=1}^{N_{tc}} T_{ci}}{N_{tc}} \quad (3)$$

Where N_{te} , N_{tc} are the number of thermocouples on the evaporator and condenser, respectively. The obtained data for temperatures and heat input rate are then used to calculate the overall heat transfer coefficient and Nusselt number as;

to calculate the overall heat transfer coefficient and Nusselt number as;

$$U = \frac{q}{\bar{T}_e - \bar{T}_c}$$

$$Nu = \frac{U \times L_1}{K_{ef}} \quad (4)$$

Where L_1 is the characteristic length, K_{ef} is the effective thermal conductivity of nanofluid, which is given by [18]

$$K_{ef} = K_m(1 + 7.47\phi) \quad (5)$$

$$L_1 = FR \times H_e \quad (6)$$

The symbols K_m , ϕ and H_e are the base fluid thermal conductivity, volume fraction of the nano-particle in the base fluid and evaporator height, respectively.

The total thermal resistance of heat pipe is given by

$$R = \frac{(\bar{T}_e - \bar{T}_c)}{Q} \quad (7)$$

One can calculate the reduction factor in total thermal resistance of heat pipe charged with nanofluid by referring its thermal resistance to that charged with pure water, expressed as

$$RR = (R_{water} - R_{nanofluid})/R_{water} \quad (8)$$

4. Result and Discussion

Experiments were performed on the considered flat heat pipe using two different working fluids; pure water and Al_2O_3 -water based nanofluid. In both cases, the effect of heat input rate Q , and filling ratio, FR on its performance are investigated. Moreover, with using nanofluid the effect of varying volume fraction of nano-particles in the base fluid, ϕ , on the thermal performance of this heat pipe is also predicted. The values of local surface temperatures along all sections of the flat heat pipe were measured ($0 \leq X \leq 300$ mm), where X is measured from the beginning of the evaporator section. $0.0 \leq X \leq 85$ mm represents the evaporator section, $85 < X \leq 200$ mm represents the adiabatic section and

$200 < X \leq 300$ mm represents the condenser section.

4.1 Results of pure water as a working fluid

Figure 3 illustrates the surface temperature along the flat heat pipe for different heat input rates (5.0, 10, 20, 30 and 40 W) at fixed filling ratio, FR of 0.45. As expected, the surface temperature decreases with increasing the distance from the evaporator, for any heat input rate. In the mean time, at a certain position along the heat pipe, the surface temperature increases with increasing heat input rate.

Figure 4 illustrates the variation of the average heat transfer coefficient, U , with the filling ratio, FR, at different heat input rates, Q . It can be noticed that, U increases with increasing FR up to a value of 0.45, where the average heat transfer coefficient starts to decrease with increasing FR. The average heat transfer coefficient, U is directly proportional to the heat input rates, Q . In other words, the small filling ratio range ($FR < 0.45$) provides little thermal resistance of the heat pipe.

Figure 5 shows the variation of the average Nusselt number, Nu , with FR, It can be noticed that Nu , increases with increasing FR, up to a value of $FR = 0.45$, where Nu tends to decrease with increasing the filling ratio. It can be also noticed that the average Nusselt number is directly proportional to the heat input rate.

4.2 Results of Al_2O_3 -water based nanofluid as a working fluid

Figure 6 illustrates the surface temperature variation along the flat heat pipe for different heat input rates, Q (5.0, 10, 20, 30 and 40 W) when using Al_2O_3 -water based nanofluid of volume fraction, $\phi = 0.5\%$ and with a fixed FR of 0.45. As expected, the surface temperature decreases with increasing the distance from the evaporator for any heat input rate. In the mean time, at a certain position along the heat pipe, the surface temperature increases with increasing the heat input rate.

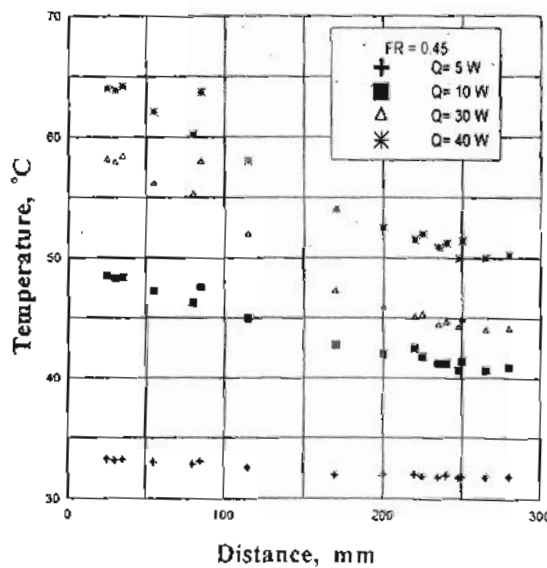


Figure 3 Temperature distribution along the flat heat pipe surface for different heat input rates

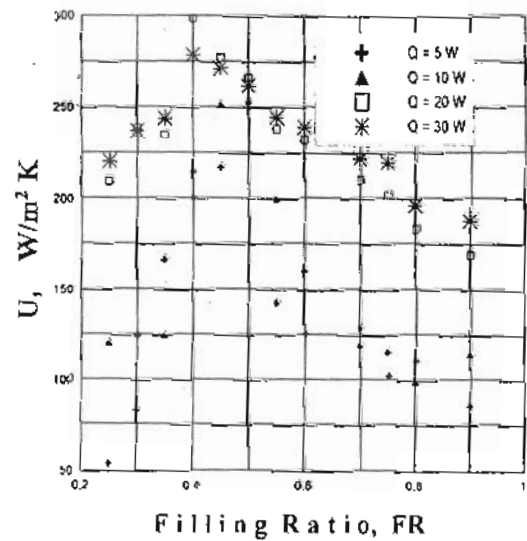


Figure 4 Variation of the average heat transfer coefficient with filling ratio at different heat input rates

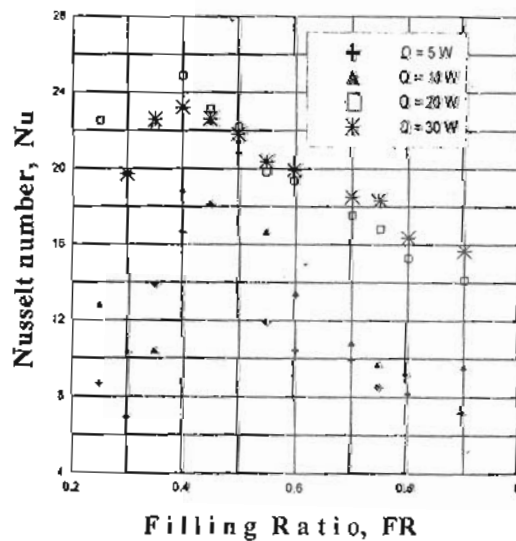


Figure 5 Variation of the average Nusselt number with filling ratio at different heat input rates

Figure 7 illustrates the variation of the average heat transfer coefficient, U with FR at different values of Q , while keeping fixed volume fraction of nano-particles ($\phi = 0.5\%$). It can be noticed that U increases with increasing the FR , up to a value of FR equals to 0.40, where Nu starts to decrease with increasing FR . It is also noticed that U gets higher values as the heat input rate, Q

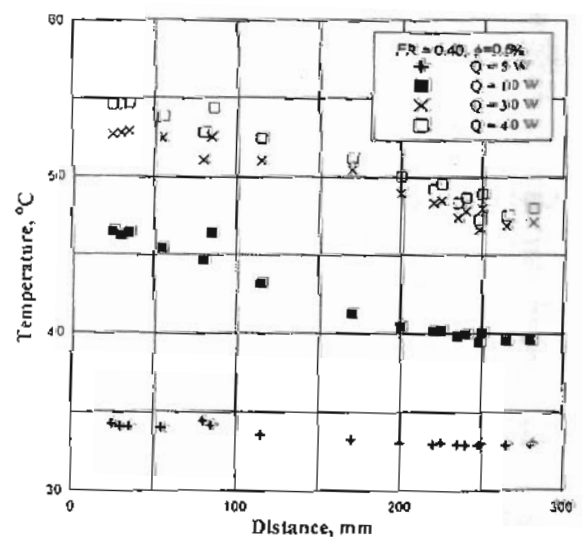


Figure 6 Temperature distribution along the flat heat pipe surface for different values of heat input rates

increases. Figure 8 shows the variation of the average Nusselt number, Nu with filling ratio, FR for Al_2O_3 -water based nanofluid of $\phi = 0.5\%$ at different heat input rate. At a certain heat input rate, the average Nusselt number is seen to be increased with increasing FR up to a value of FR equals to 0.40, where it starts to decrease. It is also noticed that the average Nusselt number increases with increasing the heat input rate.

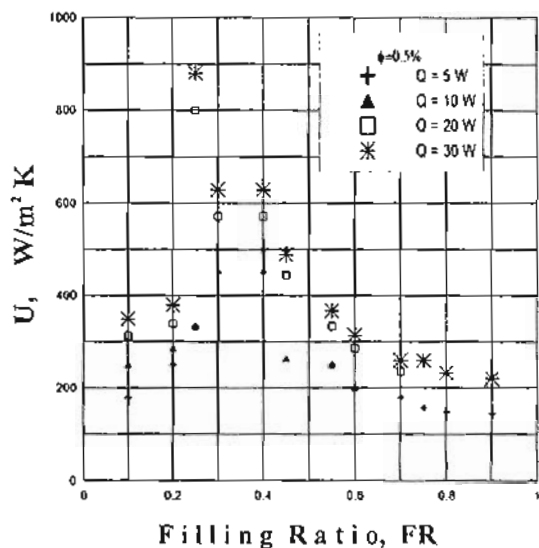


Figure 7 Variation of the average heat transfer coefficient with filling ratio at different heat input rate

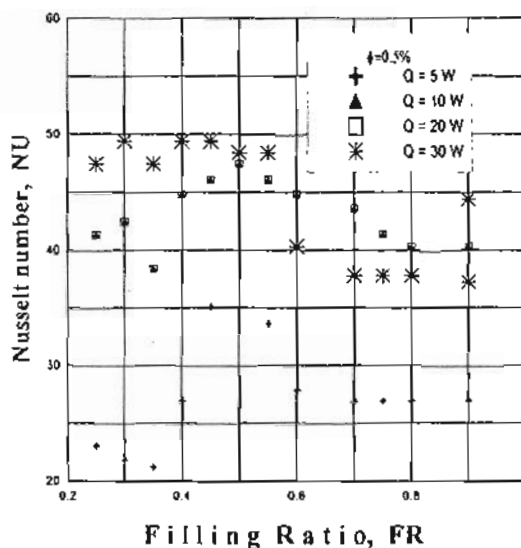


Figure 8 Variation of Nusselt number with filling ratio at different heat input rate

Figure 9 illustrates the variation of the total thermal resistance of the heat pipe, R with the filling ratio for Al_2O_3 -water based nanofluid of $\phi = 0.5\%$ at different heat input rates (10, 20, and 30 W). As shown in the figure, R decreases with the increase filling ratio up to a value of FR equals to 0.40, where its value starts to increase with increasing FR . It can be also noticed in the figure that the thermal resistance, R gets higher values as the heat input rate increases.

Figure 10 shows the variation of the total thermal resistance of the heat pipe, R with volume fraction of nano-particle in the base fluid, ϕ at two different heat input rate ($Q = 10$ W, 20W). Over the tested range of ϕ , while keeping the filling ratio of 0.45, the percentage enhancement in R ranged from 30% at $\phi = 0.5\%$ up to 28% at $\phi = 0.6\%$ compared to that when using pure water.

This is attributed to the increase of nanofluid thermal conductivity due to the presence of highly conducting nano-particles in it as well as the reduction in nanofluid viscosity. In the nanofluid literature [21], the heat transfer enhancement with nanofluids appears to go beyond the more thermal conductivity effect. In the nanofluids, this behavior is generally attributed to thermal dispersion and intensified turbulence, brought about the nano-particle motion. The dispersed nano-particles in the base fluid move homogeneously with the base fluid, so their effect on turbulence intensity can be ignored. Nanofluid properties may vary significantly within the boundary layer due to the effect of temperature gradient and thermophoresis. For a heated fluid, these effects can result in a significant decrease of viscosity within the boundary layer, thus leading to heat transfer enhancement.

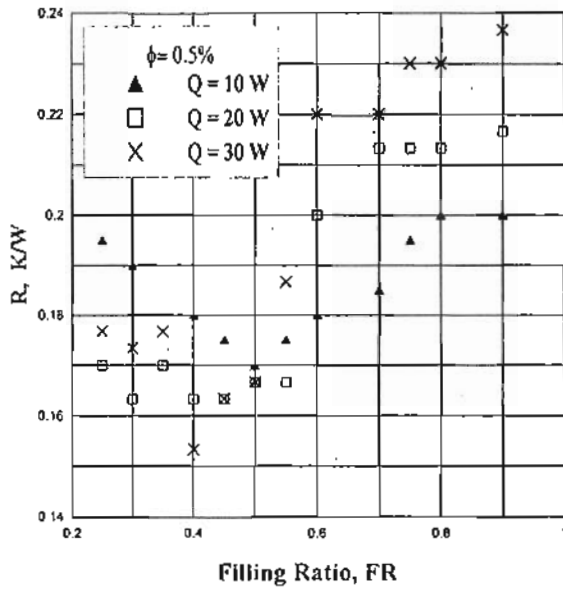


Figure 9 Variation of thermal resistance with filling ratio at different heat input rates

The effect of adding nano-particles on the thermal performance of the heat pipe is more evident if the data are expressed as a plot of the reduction rate in total thermal resistance, RR versus ϕ , as shown in figure 11. It can be observed that, the percentage reductions of R are 24%, 30%, 12%, 14%, and 13% for different ϕ of 0.25%, 0.5%, 0.6%, 0.75% and 1%, respectively. The continuing enhancement of thermal performance is observed up to ϕ equals to 0.5%, followed

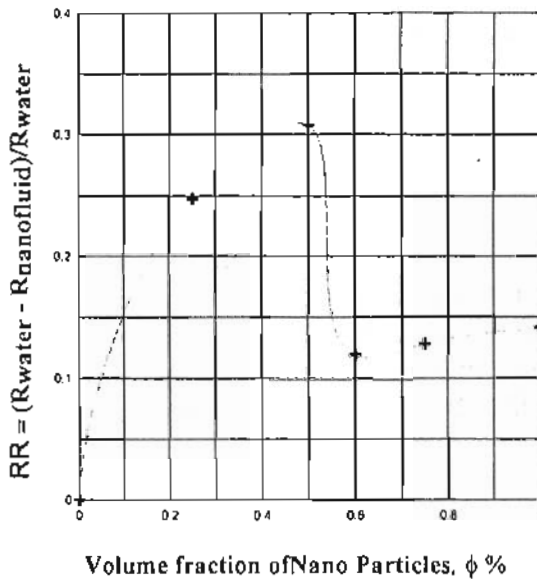


Figure 11 Reduction factor of total thermal resistance at different volume fraction of nano-particles, ϕ

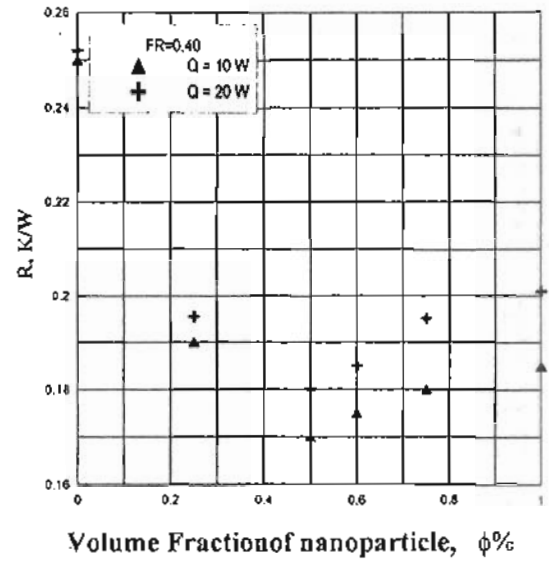


Figure 10 Variation of thermal resistance with volume fraction of nano-particles.

by a sudden reduction at ϕ equals to 0.6 %, where it starts to smoothly increase again with increasing ϕ .

The obtained heat transfer data are correlated as:

$$Nu = 3.4 [K_q^{-0.596} FR^{1.273} Pr^{-0.0532}] \quad (9)$$

The error in calculated Nusselt number is predicted by the above suggested correlation is around $\pm 15\%$, as can be seen in Fig. 12.

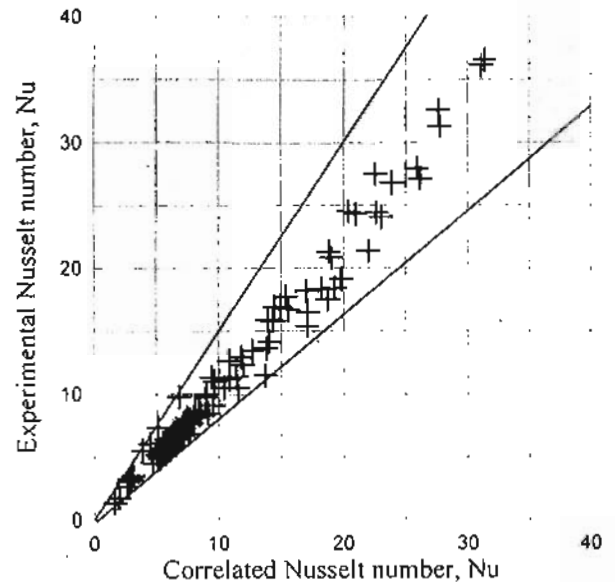


Figure 12 Experimental Nusselt number versus correlated Nusselt number over the tested range of heat input rate

4.3 Comparison with the available literature

Figure 13 shows a comparison between the present experimental results with those reported by Kang [11] in case of using pure water as a working fluid with FR equals to 0.5. It can be observed that the present experimental results for the used two working fluids have the same trend as those reported by Kang [11]. The difference between both results when using pure water may be attributed to the difference in heat pipe geometry and uncertainty in measurements.

Figure 14 shows a comparison between the present experimental results of the total

resistance, R using Al_2O_3 -water based nanofluid of $\phi = 0.5\%$ to those reported by Lips et al. [15] who used a flat heat pipe charged with n-pentane nanofluid of $\phi = 0.5\%$. One can see that the thermal resistance of the heat pipe decreases with increasing filling ratio up to a value of $FR = 0.45$, where it starts to increase with increasing the filling ratio. It can be also observed that the present experimental results a little bit higher than those reported by Lips et al [15], but have the same trend. The discrepancies in both results may be attributed to the differences in dimensions of the present tested heat pipe and his as well as due to the type of working fluid used.

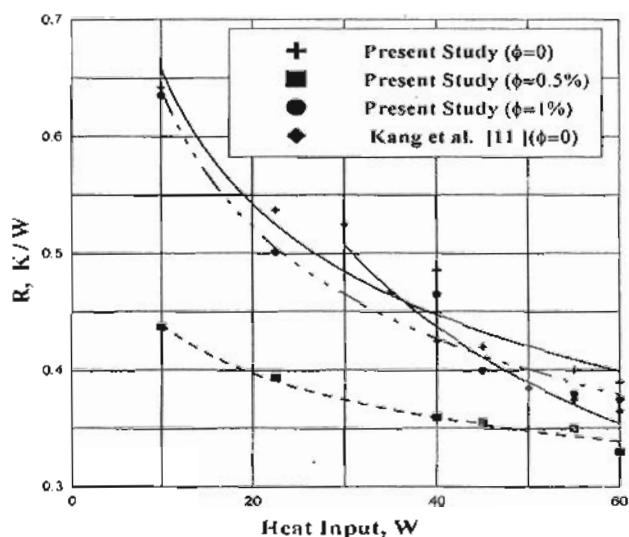


Figure 13 Comparison of the present results with available literature at different value of heat input rate

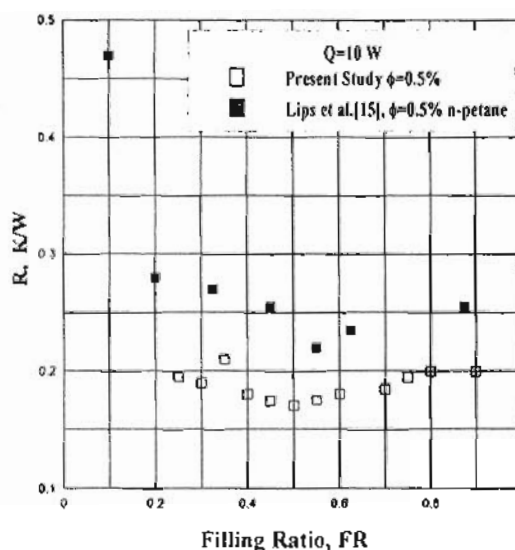


Figure 14 Comparison between present data and previous one for the variation of thermal resistance with filling ratio

5. Conclusions

Using heat pipes and based on nanofluid literature, particularly those related to the optimum operating condition, the thermal performance enhancement of such heat pipes charged with nanofluids indicates nanofluid potential as substitute for conventional fluids. This finding makes nanofluid more attractive as a cooling fluid for devices with high power intensity. A compact flat heat pipe is thermally tested with two different working fluids; pure water and Al_2O_3 -water based nanofluid. The

thermal performance of this heat pipe is predicted under different operating conditions including heat input rate, filling ratio, and volume fraction of nano-particle in water. From the obtained data and its discussion, the following conclusions may be drawn:

- 1- The optimum filling ratio of charged fluid in the tested heat pipe was about 0.45 to 0.40 for pure water as well as for Al_2O_3 -water based nanofluid, respectively.
- 2- The average heat transfer coefficient with Al_2O_3 -water nanofluid enhanced by nearly

37% at $\phi = 0.5\%$ with respect to that of pure water. The percentage enhancement reduced to nearly 10.5 % at $\phi = 0.6\%$.

3-the highest percentage reduction in thermal resistance of the tested heat pipe with Al_2O_3 - water nanofluid related to that with pure water was obtained at $\phi = 0.5\%$, after which it dramatically reduced to about 0.12 at $\phi = 0.6\%$, followed by a smooth increase with increasing the volume fraction.

4- Using nanofluids with heat pipes could lead to a major breakthrough in solid/liquid composites for numerous engineering applications such as cooling of super computers. Better ability to manage thermal properties of working fluid translates into greater energy transport, smaller and lighter thermal systems.

References

- [1] Leonard L. Vasiliev, 'Heat pipes in modern heat exchangers', *App. Thermal Eng.*, 2005, vol. 25, pp.1-19.
- [2] Babin, B. R., Peterson, G. P., and Wu, D., "Steady-state modeling and testing of a micro heat pipe", *Journal of Heat Transfer*, vol.112, 1990, pp. 595-601.
- [3] Khrustalev, D., and Faghri, A., "Thermal analysis of a micro heat pipe", *Journal of Heat Transfer*, vol. 116, 1994, pp. 189-198.
- [4] Longtin, J. P., Badran, B. and Gerner, F.M , "A one-dimensional model of a micro heat pipe during steady-state operation", *Journal of Heat Transfer*, vol. 116, 1994, pp. 709-715.
- [5] Hopkins, R., Faghri, A. and Khrustalev, D., "Flat miniature heat pipes with micro capillary grooves", *Journal of Heat Transfer*, vol. 121, 1999, pp. 102-109.
- [6] Kim, S. J., Seo, J. K. and Do, K. H., "Analytical and experimental investigation on the operational characteristics and the thermal optimization of a miniature heat pipe with a grooved wick structure", *International Journal of Heat and Mass Transfer*, vol. 46, pp. 2051-2063, 2003.
- [7] Lefèvre, F. and Lallemand, M., "Coupled thermal and hydrodynamic models of flat micro heat pipes for the cooling of multiple electronic components", *Int. J. of Heat and Mass Transfer*, vol.49, 2006, pp.1375-1383.
- [8] Revellin, R., Rullière, R., Lefèvre, F. and Bonjour, J., "Experimental validation of an analytical model for predicting the thermal and hydrodynamic capabilities of flat micro heat pipes", *Applied Thermal Engineering*, 2008.
- [9] Joung, W., Yu, T., and Lee, J., "Experimental study on the loop heat pipe with a planar bifacial wick structure", *Int. J. of Heat and Mass Transfer*, vol.51, 2008, pp. 1573- 1581.
- [10] Kaya, T., Pérez, R., Gregori, C. and Torres, A., "Numerical simulation of transient operation of loop heat pipes", *Applied Thermal Engineering*, vol.28, 2008, pp.967-974.
- [11] Kang, S. W., Wei, W. C., Tsai, S. H., and Yang, S. Y., "Experimental investigation of silver nanofluid on heat pipe thermal performance", *Applied Thermal Engineering*, vol.26, 2006, pp.2377-2382.
- [12] Pastukhov, V.G., Maidanik, Y. F., Vershinin, C.V., and Korukov, M.A., "Miniature loop heat pipes for electronics cooling", *Applied Thermal Engineering*, vol.23, 2000, pp.1125-1135.
- [13] Chang, Y. W., Cheng, C. H., Wang, J. C., and Chen, S. L., "Heat pipe for cooling of electronic equipment" *Energy Conversion and Management*, 2008.
- [14] Jouharai, H., Martinet, O., Robinson, A.J., "Experimental Study of Small Diameter Thermosyphons Charged with Water", FC-84, FC-77 & FC-3283- 5th European Thermal-Sciences Conference, The Netherlands, 2008.
- [15] Lips, S., Lefèvre, F., and Bonjour, J., "Combined effects of the filling ratio and the vapour space thickness on the performance of a flat plate heat pipe", *International*

Journal of Heat and Mass Transfer vol. 53, 2010, pp. 694–702.

[16] NanoFluid Science and Technology, Wiley Inter science, 2008.

[17]. Choi, S.U.S, "Enhancing thermal conductivity of fluids with nano-particles", in: D.A. Siginer, H.P. Wang (Eds.), Developments and Applications of Non-Newtonian Flows, in: FED, vol. 66, ASME, NY, 1995, pp. 99-103.

[18] Das, S. K., Choi, U.S., Yu,W., and Pradeep, T., "Nanofluid Science and Technology", Wiley-Interscience, 2007.

[19] Das, S. K., Putra, N., Thiesen, P., and Roetzel, W., "Temperature dependence of thermal conductivity enhancement for nanofluids", J. Heat Transfer vol.125, 2003, pp. 567-574.

[20] Lee, S., Choi, S.U.S, Li, S., and Eastman, J.A., "Measuring thermal conductivity of fluids containing oxide nano-particles," J. Heat Transfer vol. 121, 1999, pp. 280-289.

[21] You, S.M, Kim, J.H., and Kim, K.H/, Appl. Phys. Lett.,vol., 83, 2003, pp. 3374-3376.